Chin. J. Astron. Astrophys. Vol. 6 (2006), No. 6, 733–740
(*http://www.chjaa.org*)

Chinese Journal of
Astronomy and
Astrophysics

Solar Impulsive Hard X-Ray Emission and Two-Stage Electron Acceleration

Tian-Xi Zhang[1,2], Arjun Tan[1] and Shi Tsan Wu[2]

[1] Physics Department, Alabama A & M University, Normal, AL 35762, USA
tianxi.zhang@email.aamu.edu
[2] Center for Space Plasma and Aeronomic Research, The University of Alabama in Huntsville, AL 35899, USA

Received 2005 December 23; accepted 2006 June 8

Abstract Heating and acceleration of electrons in solar impulsive hard X-ray (HXR) flares are studied according to the two-stage acceleration model developed by Zhang for solar ^{3}He-rich events. It is shown that electrostatic H-cyclotron waves can be excited at a parallel phase velocity less than about the electron thermal velocity and thus can significantly heat the electrons (up to 40 MK) through Landau resonance. The preheated electrons with velocities above a threshold are further accelerated to high energies in the flare-acceleration process. The flare-produced electron spectrum is obtained and shown to be thermal at low energies and power law at high energies. In the non-thermal energy range, the spectrum can be double power law if the spectral power index is energy dependent or related. The electron energy spectrum obtained by this study agrees quantitatively with the result derived from the Reuven Ramaty High Energy Solar Spectroscopic Imager (RHESSI) HXR observations in the flare of 2002 July 23. The total flux and energy flux of electrons accelerated in the solar flare also agree with the measurements.

Key words: acceleration of particles – instabilities – plasmas – Sun: flares – Sun: particle emission – Sun: X-ray

1 INTRODUCTION

Recent observations of the solar flare of 2002 July 23 by the Reuven Ramaty High Energy Solar Spectroscopic Imager (RHESSI) have shown that the impulsive hard X-ray (HXR) spectrum $I(\epsilon)$ (ϵ is the photon energy) includes a superhot thermal component with temperatures up to ~ 40 MK and a non-thermal (usually double) power-law component with energies above tens of keV (Lin et al. 2003; Emslie et al. 2003). This result implies that electrons undergo two energization processes (i.e., heating and acceleration) before they target footpoints to emit HXRs. In the heating process, the electrons are extremely heated up to ~ 40 MK with a thermal spectrum; while in the acceleration process, electrons in the distribution tail are accelerated to tens of keV (or higher) with a double power-law spectrum.

From $I(\epsilon)$ measured in the time interval 00:30:00-00:30:20, the mean source electron spectrum $\bar{F}(E)$ (E the electron energy) was derived (Holman et al. 2003; Piana et al. 2003). Using the forward-fitting algorithm, Holman et al. (2003) obtained a double power-law $\bar{F}(E)$ with a break (i.e., slope change) at $E_b =$ 129 keV in the non-thermal energy range. In the low-energy range, $\bar{F}(E)$ was assumed to be isothermal. In terms of the regularized-inversion algorithm, Piana et al. (2003) obtained $\bar{F}(E)$ at both low and high energies. In the non-thermal energy range, $\bar{F}(E)$ is also double power law but has a big energy break and cutoff ($E_b \sim 160$ and $E_c \sim 50$). In the low energy range, $\bar{F}(E)$ was found having a significant deviation from isothermal.

A relation between $\bar{F}(E)$ and the injected electron spectrum $F_0(E)$ was derived by Emslie (2003). For a cold target, we have $F_0(E) \propto \bar{F}(E)E^{-2}[1 - d\ln \bar{F}(E)/d\ln E]$, in which the energy factor causes $F_0(E)$ to be quite different from $\bar{F}(E)$. $F_0(E)$ is much smaller than $\bar{F}(E)$ but has a larger spectral power index. Brown et al. (2003) indicated that a power law $F_0(E) \propto E^{-\gamma}$ corresponds to a power law $\bar{F}(E) \propto E^{-\gamma+2}$ at small and large E/E_*, where E_* is a reference energy between E_c and E_b (Kontar et al. 2003). Near E_*, however, $\bar{F}(E)$ flattens by up to about half a unit in the index. Thus, in the non-thermal energy range, a double power-law $\bar{F}(E)$ usually relates to a double power-law $F_0(E)$ with a larger spectral power index. The slope change should be less in $F_0(E)$ than in $\bar{F}(E)$ because $\bar{F}(E)$ flattens near E_*. In the thermal-energy range, $F_0(E)$ is also expected to significantly derivate from $\bar{F}(E)$ as pointed out by Piana et al. (2003).

The injected electron spectrum $F_0(E)$ is equivalent to the flare-produced electron spectrum $F_1(E)$, which can be determined according to flare-acceleration mechanisms. Studying $F_1(E)$ based on a flare-acceleration mechanism and comparing $F_1(E)$ with $F_0(E)$ are helpful to understand the processes of electron accelerations in solar flares and HXR emissions from sources. To obtain a flare-produced electron spectrum that corresponds to the solar impulsive HXR spectrum measured by RHESSI, the flare-acceleration mechanism should involve both the heating and acceleration of electrons and give a double power-law electron spectrum.

Cartwright & Mogro-Campero (1972) proposed a two-stage acceleration scenario for solar flares: a first stage involving a particle-heating process and a second stage in which particles that have been preheated above a certain threshold (Sturrock 1974) are further accelerated to high energies in flare-acceleration processes such as Fermi acceleration as suggested by Fisk (1978). Based on the Cartwright & Mogro-Campero's scenario and Fisk's work, Zhang (1995, 1999) completed the development of the two-stage acceleration model and gave self-consistent explanation of various aspects of heating and accelerations of ^{3}He, electrons, and heavy ions in solar ^{3}He-rich events (Zhang 2003a, b, 2004; Zhang & Wang 2003, 2004; Zhang et al. 2005a; for observations see Luhn et al. 1987; Mason et al. 2002, 2004; Reames et al. 1994; Reames & Ng 2004).

In this paper, the two-stage acceleration model is applied to investigate the heating and acceleration of electrons in solar superhot impulsive HXR flares. The flare-produced electron spectrum $F_1(E)$ is determined at both low and high energies and compared with $F_0(E)$ and $\bar{F}(E)$ that are derived from the RHESSI HXR spectrum $I(\epsilon)$. The total flux $J_1(E_1)$ and energy flux $F_{1E}(E_1)$ of electrons with energies greater than a reference E_1 are also calculated and compared with the measurements.

2 ELECTRON HEATING BY H-CYCLOTRON WAVES

In a multi-ion plasma consisting of electrons, H, ^{4}He, ^{3}He, and heavy ions with the coronal composition, electric currents (aligned on or across the field) can, if strong enough, excite electrostatic ion-cyclotron waves. Along-field currents can be generated in the solar corona because of photospheric convection, twisted magnetic fields, or electron beams (Fisk 1978; Temerin & Roth 1992; Miller & Vinas 1993; Zhang 1995). Across-field currents can be generated in the solar corona by global MHD modes (Markovskii 2001; Zhang 2003b). The dispersion relation of current-driven, electrostatic ion-cyclotron waves is given by (Kindel & Kennel 1971; Fisk 1978; Zhang 1995, 1999),

$$1 + \sum_{\sigma} \frac{1}{k^2 \lambda_{\mathrm{D},\sigma}^2} \left[1 + \sum_{n=-\infty}^{n=\infty} \frac{\omega - \boldsymbol{k}\cdot\boldsymbol{v}_{d,\sigma}}{\sqrt{2}k_\parallel v_{T,\sigma}} Z\left(\frac{\omega - \boldsymbol{k}\cdot\boldsymbol{v}_{d,\sigma} - n\Omega_\sigma}{\sqrt{2}k_\parallel v_{T,\sigma}} \right) \Gamma_n(\mu_\sigma) \right] = 0, \tag{1}$$

where subscript σ refers to the particle species; ω is the frequency with real part ω_r and imaginary part ω_i; $\boldsymbol{k}$ is the wavenumber vector with perpendicular component $k_\perp$ and parallel component $k_\parallel$; $v_{T,\sigma} = (T_\sigma/m_\sigma)^{1/2}$ is the thermal speed with T_σ the temperature and m_σ the mass; $\lambda_{\mathrm{D},\sigma} = [T_\sigma/4\pi n_{\sigma,0}(Z_\sigma^* e)^2]^{1/2}$ is the Debye length with Z_σ^* the charge state ($Z_e^* = -1$) and $n_{\sigma,0}$ the initial number density; $\Omega_\sigma = Z_\sigma^* eB/m_\sigma$ is the cyclotron frequency with e the proton electric charge and B the background magnetic field; $\boldsymbol{v}_{d,\sigma}$ is the current velocity, which is zero for ions and is denoted by $\boldsymbol{v}_d$ for electrons; Z is the plasma-dispersion function (Fried & Conte 1961); $\Gamma_n(\mu_\sigma)$ is defined by $\Gamma_n(\mu_\sigma) = I_n(\mu_\sigma)\exp(-\mu_\sigma)$ with I_n the modified Bessel function of the n^{th} order; and μ_σ is defined by $\mu_\sigma = k_\perp^2 \rho_{T,\sigma}^2$ with $\rho_{T,\sigma} = v_{T,\sigma}/\Omega_\sigma$ the gyro-radius of a thermal particle.

Figure 1(a) shows the dispersion relation of H-cyclotron waves (i.e., real frequency versus the perpendicular wavenumber with the parallel wavenumber being fixed at $k_{\|}\rho_{^4\mathrm{He}} = 0.08$) for three cases of $T_e/T_{\mathrm{H}} = 1$, 2.5 and 5. The other initial parameters are chosen based on the coronal plasma properties including $n_{^4\mathrm{He},0}/n_{\mathrm{H},0} = 0.1$, $T_{\mathrm{H}} = T_j$ with j representing ion species excluding H, $\omega_{pe}/\Omega_e = 1$ (an insensitive parameter) with ω_{pe} the plasma frequency. In this paper, we consider an along-field current and the current velocity is chosen as $v_d/v_{T,e} = 0.56$, 0.28 and 0.20, respectively. The effects of heavy ions on the H-cyclotron waves have been neglected because the abundances of heavy ions are low. The results show that in all three cases the parallel phase velocities of unstable (or growing) H-cyclotron waves are $\omega_{\mathrm{Re,H}}/k_{\|} \sim (30-40)v_{T,^4\mathrm{He}} \sim (0.3-0.5)v_{T,e} \lesssim v_{T,e}$. This means that electrons with velocities $v_{\|} \lesssim v_{T,e}$ can satisfy well the Landau-resonance condition $\omega - k_{\|}v_{\|} = 0$ and thus be significantly heated by H-cyclotron waves through Landau resonance. In addition, protons are generally heated due to the non-resonant dissipation (Zhang 1995, 1999).

When an electrostatic H-cyclotron wave is excited, it resonates with the thermal particles, it alters the particle distribution, which is initially assumed to be Maxwellian, and thus increases the temperature. The heating of particles by electrostatic ion-cyclotron waves was studied in the fluid framework by Palmadesso et al. (1974) and Fisk (1978). Palmadesso et al. (1974) focused on the non-resonant heating by electrostatic turbulence and Fisk (1978) also included the resonant heating by ^{4}He-cyclotron waves (see also Kocharov & Kocharov 1984). In terms of the conventional quasilinear kinetic analysis, Zhang (1995, 1999) derived the equivalent heating rate expressions for the current-driven H-cyclotron waves. From the quasilinear theory of particle-wave interaction, the wave varies the distribution a little bit in each time step or gyro-period of ions. The rate of variation of the distribution by ion-cyclotron waves is given by a complicated equation (see eq. (A3) in Zhang 1995), which is obviously not Maxwellian (for Alfvén waves, see Zhang & Li 2004; Zhang et al. 2005b). Integrating the rate of variation of the distribution, we have the heating rates of electrons due to Landau resonance and protons due to non-resonant dissipation as (Fisk 1978; Zhang 1995, 1999),

$$\frac{1}{T_e}\frac{dT_e}{dt} = \frac{16\sqrt{\pi}}{3}\left(\frac{T_{\mathrm{H}}}{T_e}\right)^2\left(\frac{\omega_{\mathrm{Re,H}}}{\Omega_{\mathrm{H}}}\right)^2\frac{(\omega_{\mathrm{Re,H}}-\Omega_{\mathrm{H}})^2}{\sqrt{2}k_{\|}v_{T,e}}\exp\left[-\left(\frac{\omega_{\mathrm{Re,H}}}{\sqrt{2}k_{\|}v_{T,e}}\right)^2\right], \tag{2}$$

$$\frac{1}{T_{\mathrm{H}}}\frac{dT_{\mathrm{H}}}{dt} = \frac{16}{3}I_1(\mu_{\mathrm{H}})\exp(-\mu_{\mathrm{H}})\omega_{\mathrm{Im,H}}. \tag{3}$$

It is seen that the heating of electrons depends explicitly on m_e, T_e, T_{H}, $\omega_{\mathrm{Re,H}}$, and $k_{\|}$. The most important point is whether or not the Landau-resonance condition is well satisfied. If most of the particles satisfy the Landau-resonance condition, the argument in the exponential function of Equation (2) will be small. In this situation, an efficient heating of electrons is possible. The heating of H is proportional to the growth rate $\omega_{\mathrm{Im,H}}$ and is thus generally weak. Preheating of particles by the ion-cyclotron waves generated by the electron drift or electric currents is assumed to occur before the second stage acceleration, at the occurrence of magnetic reconnection process.

Figure 1(b) shows the heating of electrons (solid lines) and protons (dotted lines) by the H-cyclotron waves in the three cases shown in Figure 1(a). In the calculation, the most unstable modes are considered and the dispersion properties are chosen as $\omega_r/\Omega_{^4\mathrm{He}} = 2.4$, 2.56 and 2.72 and $k_{\|}\rho_{^4\mathrm{He}} = 0.08$. It is seen that the electron temperature increases by a factor of 20–30 in about 300 H gyro-periods, or $\sim 3\times 10^{-3}$ second if $B_0 = 10$ Gauss. If the initial electron temperature in the background is ~ 1.5–2 MK, then H-cyclotron waves can quickly heat the electrons up to ~ 40 MK – the order of RHESSI measurements in the solar flare of 2002 July 23.

3 ELECTRON ACCELERATION AND ENERGY SPECTRUM

Preheated electrons with velocities above a threshold can be accelerated when a relative motion between the magnetic field lines and a plasma flow/shock exists. The electric field $\boldsymbol{E}$ for the acceleration is given by $\boldsymbol{E} = -\boldsymbol{U}\times\boldsymbol{B}$, where $\boldsymbol{U}$ is the velocity of the relative motion. This acceleration is usually called the drift-shock or first-order (classical) Fermi acceleration and has a time scale less than one second. It is a popular flare-acceleration mechanism and has been extensively studied (Fermi 1949; Parker 1957; Jokipii 1966; Sakurai 1974; Ramaty 1979; Möbius et al. 1980; Masuda et al. 1994; Tsuneta & Naito 1998; Aschwanden 2002).

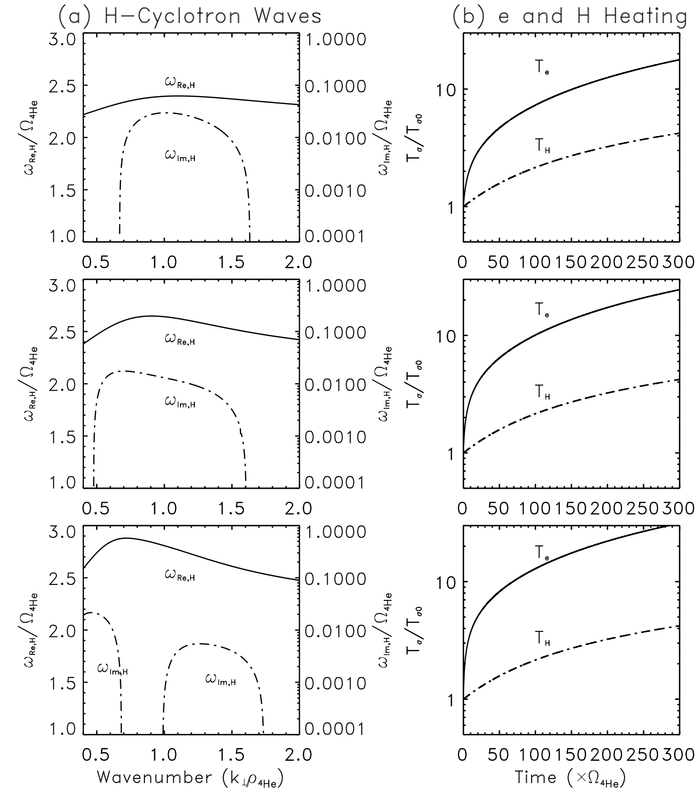

Fig. 1 (a) Dispersion relation of H-cyclotron waves in three cases of $T_e/T_{\rm H} = 1$ (Top), 2.5 (middle), and 5 (low). The drift velocities for the three cases are $v_d/v_{T,e} = 0.2$, 0.43 and 0.56, respectively. (b) Heating of electrons by the unstable H-cyclotron waves in the three cases.

The distribution of high-energy electrons due to the Fermi acceleration was derived by Zhang (1995, 1999, 2003a). Over the entire energy range, the distribution in terms of the kinetic energy $E = 1/2m\,_e v^2$ can be approximately represented by

$$f_e(E) \simeq n_{e,0}\left(\frac{1}{2\pi v_{T,e}^2}\right)^{3/2}\exp\left(\frac{-E}{m_e v_{T,e}^2}\right) +$$
$$n_{e,0}\frac{1-\nu}{2\pi\sqrt{\pi}}\left(\frac{m_e}{2}\right)^{(4-\nu)/2} v_{\rm thr}^{(1-\nu)}\exp\left(-\sqrt{\frac{m_e v_{T,e}^2}{2E}} - \frac{v_{\rm thr}^2}{2v_{T,e}^2}\right)\times$$
$$\left[\frac{\sqrt{\pi}}{2}\sum_{m=1}^{3} a_m\left(1+0.332\frac{v_{\rm thr}}{v_{T,e}}\right)^{-m} + \frac{v_{\rm thr}}{\sqrt{2}v_{T,e}}\right]E^{(\nu-4)/2}, \quad (4)$$

where ν is the exponent of the power spectrum of magnetic fluctuation (Möbius et al. 1980); a_m with $m = 1, 2, 3$ represents three constants $a_1 = 0.348$, $a_2 = -0.096$ and $a_3 = 0.748$ (Abramowitz & Stegun 1970); and $v_{\rm thr}$ is the threshold velocity of electrons for the acceleration, which is determined from the condition $\rho_e \gtrsim l_{e,c}$, where ρ_e is the gyro-radius of an electron with a velocity v_e and $l_{e,c}$ is a characteristic (or critical) length for the second-stage acceleration (Sturrock 1974; Möbius et al. 1980). The first term of Equation (4) corresponds to the low-energy thermal component (Maxwellian distribution) and the second term corresponds to the accelerated component (approximately power law). We should note that Equation (4) is obtained from $f(v)$ by replacing $v = \sqrt{2E/m_e}$.

The number density of electrons with velocities between v and $v + dv$ is given by

$$dn_e(v) = f_e(v) 4\pi v^2 dv, \tag{5}$$

where $f_e(v)$ is the distribution in terms of the velocity and dv is a small velocity interval. In terms of E, the flux of electrons with energies between E and $E + dE$ is given by

$$dJ_e(E) = dn_e(v)v = \frac{8\pi}{m_e^2} E f_e(E) dE. \tag{6}$$

Then the differential flux (denoted by $F_1(E)$) of electrons is represented as

$$F_1(E) \equiv \frac{dJ_e(E)}{dE} = \frac{8\pi}{m_e^2} E f_e(E). \tag{7}$$

It is seen that, at $E < E_{\text{thr}}$, the thermal electron flux dominates: ($F_1(E) \propto E \exp(-E/2E_{T,e})$); while at $E > E_{\text{thr}}$, the power-law electron flux dominates: ($F_1(E) \propto E^{-\gamma}$). Here $E_{\text{thr}} = m_e v_{\text{thr}}^2/2$ is the threshold energy, $E_{T,e} = m_e v_{T,e}^2/2$ is the electron thermal energy, and $\gamma = 1 - \nu/2$ is the spectral power index. The flare-produced electron flux/spectrum depends on E_{thr}, T_e and γ.

The energy spectrum of electrons depends on three key parameters: the spectral power index, electron temperature, and threshold energy, which have clear physical meanings (Möbius et al. 1980; Zhang 1995; Masuda et al. 1998; Aschwanden 2002). If the spectral power index γ is constant, the flare-produced electron spectrum is thermal at low energies and single power law at high energies. To have a flare-produced electron spectrum in the form of a double power-law, the spectral power index should be energy dependent or related (Zhang & Wang 2004). Assuming the spectral power index γ to be a constant γ_0 when $E \leq E_b$ and energy dependent in the following form when $E > E_b$,

$$\gamma = \gamma_0 + \alpha E_b \left[1 - \left(\frac{E_b}{E}\right)^\beta\right], \tag{8}$$

we have a double power-law flare-produced electron spectrum. Here α and β are two constants that determine how much the slope changes; E_b is the break energy in keV at which the slope changes. If either α or β is zero, the spectrum becomes single power law (i.e., no slope change). A simple addition of two single power-laws with two constant spectral power indices does not result in a double power-law, as we expected.

Figure 2 shows the flare-produced electron spectrum – the differential flux (in units of electrons cm $^{-2}$ s^{-1} keV^{-1}) of electrons accelerated in the solar flare as a function of the electron energy (in units of keV). In the impulsive phase, especially in the time interval 00:30:00 –00:30:20, the electron temperature is in the range of 35 MK $\lesssim T_e \lesssim$ 45 MK (Lin et al. 2003; Emslie et al. 2003; Holman et al. 2003). Figure 2(a) and (b) correspond to two chosen values of the temperature of preheated electrons (38 and 42 MK), and three values of the spectral power index γ_0 at $E \leq E_b$ (2.5, 3.0, 3.5). The chosen empirical constants are $\alpha = 0.02$ and $\beta = 0.5$. The threshold energy (i.e., the energy separating the thermal component from the power law component or the energy cutoff E_c) is set at $E_{\text{thr}} \simeq 40$ keV, which corresponds to $v_{\text{thr}} = 4.25 v_{T,e}$. The break energy is chosen as $E_b = 129$ keV, as given by Holman et al. (2003). The electron density in the flare is chosen as $n_{e,0} = 6 \times 10^8 \text{cm}^{-3}$ (Aschwanden 2002).

It can be found from Figure 2 that $F_1(E)$ is composed of two electron components in the flux: a thermal component at low energies and a double power-law component at high energies. The general trend of $F_1(E)$ is similar to that of $\bar{F}(E)$ fitted to, or inverted from the RHESSI observed HXR spectrum by Holman et al. (2003) or Piana et al. (2003). The values of the flare-produced electron flux are less than the mean source electron flux by a factor of $10^{-2} - 10^{-3}$ if the mean source density is $\bar{n} = 6 \times 10^{10} \text{cm}^{-3}$ and the source emitting volume is $V = 4 \times 10^{27} \text{cm}^3$ as given by Lin et al. (2003). According to the relation between $F_0(E)$ and $\bar{F}(E)$ (Emslie 2003), we have $F_0(E_1)/\bar{F}(E_1) \lesssim 10^{-2}$ for a cold target, $E_1 = 100$ keV and the flare area $A \gtrsim 10^{18} \text{cm}^2$. Thus, $F_1(E)$ obtained by this study agrees well with $F_0(E)$.

The total energy flux (in units of erg s^{-1}) and total flux (in units of electron s^{-1}) of electrons produced in the solar flare with energies above E_1 are given by $F_{1E}(E_1) = A \int_{E_1}^{\infty} E F_1(E) dE$ and $J_1(E_1) = A \int_{E_1}^{\infty} F_1(E) dE$, respectively. Table 1 shows the values of $F_{1E}(E_1)$ and $J_1(E_1)$ with E_1 above

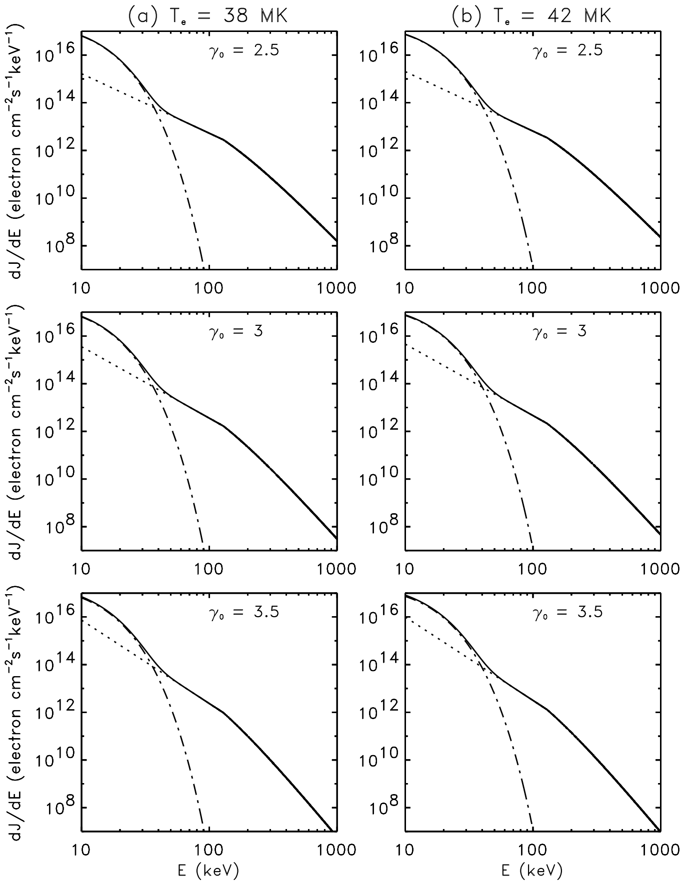

Fig. 2 Flare-produced electron spectrum for two values of T_e (38 and 42 MK) and three values of the spectral power index γ_0 (2.5, 3.0, 3.5).

Table 1 Total energy flux and total flux of electrons with energies above 10, 20 and 100 keV.

E_1 (keV)	$F_{1E}(E_1)$ (erg s^{-1})	$J_1(E_1)$ (electrons s^{-1})
10	10^{29}	4×10^{36}
20	2×10^{28}	4×10^{35}
100	8×10^{26}	3×10^{33}

10, 20 and 100 keV. The values in Table 1 are proportional to A and $n_{e,0}$, which were chosen as $A = 10^{19}$ cm^2 and $n_{e,0} = 6 \times 10^8$ cm^{-3}. Observations show that the rate of energy deposition by the accelerated electrons with energies above 20 keV is $\sim 1 - 2 \times 10^{28}$ erg s^{-1} in the impulsive phase (Lin et al. 2003; Holman et al. 2003), which agrees with the energy flux of flare-produced electrons given in Table 1. For a cold target, the total energy flux of injected electrons with energies above 100 keV is $\sim 1 - 10 \times 10^{26}$ erg s^{-1}, which also agrees with the energy flux of electrons given in Table 1. The total flux of electrons with energies above 10 keV given in Table 1 is in the range given by Holman et al. (2003).

For different impulsive flares, the energy range of nonthermal electrons and the temperature of thermal electrons may be different in the flare-produced electron spectra. According to the two-stage acceleration model, the energy range of nonthermal particles is determined by the threshold energy, the minimum energy for the particles to be injected into the flare acceleration process. For instances, if the threshold energy is about 15 keV, then electrons with energies above 15 keV are nonthermal as RHESSI recently observed (Caspi et al. 2005). If the threshold energy is about 50 keV, then the electrons with energies above 50 keV are nonthermal as RHESSI observed in the 2002 July 23 flares (Lin et al. 2003). The condition that the energy-gain rate is greater than the energy-loss rate (for the collisional energy loss for the second stage acceleration, see equation (1) of Tsuneta & Naito (1998), while the preheating process is usually assumed to be collisionless) can be used to determine the threshold energy for the second stage acceleration. The preheating process is usually assumed collisionless. As shown by Masuda et al. (1994) and Tsuneta & Naito (1998), the threshold energy for electrons relates to the angle of the drift-shock normal. The temperature of thermal electrons depends on the power and dispersion relations of the excited ion-cyclotron waves. In the impulsive flares, thermal or nonthermal electrons produce thermal or nonthermal Hard X-rays.

The Fermi acceleration time scale was obtained as 0.3 to 0.6 second by Tsuneta & Naito (1998). In the two-stage acceleration model, the acceleration time is the time of preheating, which is much shorter than a second, plus the time of the Fermi acceleration. The sum is less than the order of one second. For the stochastic acceleration, the time scale is also around the order of one second (Miller & Vinas 1993; Liu et al. 2004). Therefore, the two-stage acceleration is on the same time scale as the stochastic acceleration in solar flares. On the other hand, the direct electric field acceleration may cause charge separation, which decreases the electric field strength and hence the acceleration efficiency.

4 DISCUSSION AND CONCLUSIONS

Hard X-ray radiation during solar impulsive flares is generally thought to be due to electron-ion bremsstrahlung (Lin et al. 1981). Accelerated or fast electrons emit X-rays when they interact with plasma ions of a relatively cool solar atmosphere, for instance, at the foot points. The thermal emission comes mostly from the plasma at the loop top, either evaporated from the foot points or heated directly in the corona and flare (Lin et al. 2003; Liu et al. 2004). In this two-stage acceleration model, we have not specified the details on the source and the field configuration (Masuda 1994). Our studies are to focus on the heating and acceleration of electrons in solar impulsive flares and on a possible mechanism for the energetic particles to have a double power law spectrum.

To obtain a double-power-law energy spectrum of electrons, we have, from empirical evidence, suggested that the spectral power index is dependent on the electron energy. In a solar impulsive event, variation in the magnetic fluctuation can cause changes in the spectral power index (Möbius et al. 1980). In general, this variation is different at different times and locations. Electrons are accelerated to different levels of energy when the magnetic fluctuation is different. Therefore, it is natural to consider the spectral power index to be energy related. The empirical model is an empirical formulation of the relation. At present, the measurements for the energy spectrum of electrons from impulsive events are quite limited: they are not enough to determine the physics that underlies the slope change.

The flare-produced electron spectrum obtained with the two-stage acceleration model depends on the electron temperature, the spectral power index, and the threshold energy (or the energy cutoff), which vary temporally/transiently during the solar flare (Holman et al. 2003). Choosing a temperature, a spectral power index and an energy cutoff as given by Holman et al. (2003) from the RHESSI observations, we can estimate the flux of electrons accelerated in solar flares at different times. A lower energy cutoff implies more electrons are accelerated, which agrees with the result shown by Holman et al. (2003) that the maximum of electron flux corresponds to the minimum energy cutoff in the rise phase. In this letter, we have numerically studied two exemplar cases with $T_e = 38$ and 42 MK in the impulsive phase. We did not calculate the electron flux in the rise phase because the rise phase may involve a different acceleration mechanism from the impulsive phase. Lin et al. (2003) indicated that the impulsive phase acceleration is related to magnetic reconnection. In addition, the mean source electron flux was derived also for the impulsive phase. We leave a study of the electron flux in the rise phase to the future.

To summarize, we have studied the heating and acceleration of electrons in solar impulsive hard X-ray flares according to the two-stage acceleration model developed by Zhang (1995, 1999). The flare-produced electron spectrum obtained by this study includes a thermal component and a non-thermal power-law component. The non-thermal component is single power law if the spectral power index is a constant, and can be double power law if the spectral power index is energy dependent. The results are compared with the injected electron spectrum and the mean source electron spectrum related to (or derived from) the RHESSI HXR observations. Qualitatively, $F_1(E)$ agrees very well with $F_0(E)$ and both are much smaller than $\bar{F}(E)$ due to the electron density in being much lower in the flare site than in the source. The total flux and energy flux obtained for the electrons accelerated in the solar flare also agree with the measurements.

Acknowledgements The work was supported by NASA Grant (NNG04GD59G A/C 2-302-14-3380-119) and National Science Foundation (ATM 00-70385). TXZ is grateful to Dr. A. G. Emslie and R. P. Lin for taking time to read the manuscript of this paper.

References

Abramowitz M., Stegun I. A., 1970, Handbook of Mathematical Functions, New York: Dover
Aschwanden M. J., 2002, Space Sci. Rev., 101, 1
Brown J. C., Emslie A. G., Kontar E. P., 2003, ApJ, 595, L115
Caspi A., Krucker S., Lin R. P., 2005, AGU Fall Meeting, SH13A-0285
Cartwright B. G., Mogro-Campero A., 1972, ApJ, 177, L43
Emslie A. G., 2003, ApJ, 595, L119
Emslie A. G., Kontar E. P., Krucker S., Lin R. P., 2003, ApJ, 595, L107
Fermi E., 1949, Phys. Rev., 75, 1169
Fisk L. A., 1978, ApJ, 224, 1048
Fried B. D., Conte S. D., 1961, The Plasma Dispersion Function, New York: Academic
Holman G. D., Sui L., Schwartz R. D., Emslie A. G., 2003, ApJ, 595, L97
Jokipii J. R., 1966, ApJ, 143, 961
Kindel J. M., Kennel C. F., 1971, J. Geophys. Res., 76, 3055
Kontar E. P. et al., 2003, ApJ, 595, L123
Kocharov L. G., Kocharov G. E., 1984, Space Sci. Rev., 38, 89
Lin R. P., Schwarts R. A., Pelling R. M., Hurley K. C., 1981, ApJ, 251, L109
Lin R. P. et al., 2003, ApJ, 595, L69
Liu W., Jiang Y. W., Liu S. et al., 2004, ApJ, 611, L53
Luhn A., Klecker B., Hovestadt D., Möbius E., 1987, ApJ, 317, 951
Markovskii S. A., 2001, ApJ, 557, 337
Mason G. M., Mazur J. E., Dwyer J. R., 2002, ApJ, 565, L51
Mason G. M., Mazur J. E., Dwyer J. R. et al., 2004, ApJ, 606, 555
Masuda S., Kosugi T., Hara H. et al., 1994, Nature, 371, 495
Masuda S., 1994, Dissertation (Yohkoh HXT group, Tokyo)
Miller J. A., Vinas A. F., 1993, ApJ, 412, 386
Möbius E., Hovestadt D., Klecker B. et al., 1980, ApJ, 238, 768
Palmadesso P. J., Coffey T. P., Ossakow S. L., Papadopoulos K., 1974, GRL, 1, 105
Parker E. N., 1957, Phys. Rev., 107, 830
Piana M., Massone A. M., Kontar E. P. et al., 2003, ApJ, 595, L127
Ramaty R., 1979, in Particle Acceleration Mechanisms in Astrophysics, eds., J. Arons, C. Max, C. McKee, New York: AIP, p.135
Reames D. V., Meyer J. P., von Rosenvinge T. T., 1994, ApJS, 90, 649
Reames D. V., Ng C. K., 2004, ApJ, 610, 510
Sakurai K., 1974, Ap&SS, 28, 375
Sturrock P. A., 1974, in IAU Symp. 57, Coronal Disturbances, ed., G. Newkirk, Jr., Dordrecht: Reidel, p.437
Temerin M., Roth I., 1992, ApJ, 391, L105
Tsuneta S., Naito T., 1998, ApJ, 495, L67
Zhang T. X., 1995, ApJ, 449, 916
Zhang T. X., 1999, ApJ, 518, 954
Zhang T. X., 2003a, J. Geophys. Res., 108, 1031
Zhang T. X., 2003b, ApJ, 597, L69
Zhang T. X., Li B., 2004, Phys. Plasmas, 11, 2172
Zhang T. X., Wang J. X., 2003, ApJ, 588, L57
Zhang T. X., Wang J. X., 2004, ApJ, 613, L165
Zhang T. X., Wang J. X., Tan A., 2005a, J. Geophys. Res., 110, A1211
Zhang T. X., Wang J. X., Xiao C. J., 2005b, Chin. J. Astron. Astrophys. (ChJAA), 5, 285